

Supplemental figures and figure legends

Supplemental figure 1:

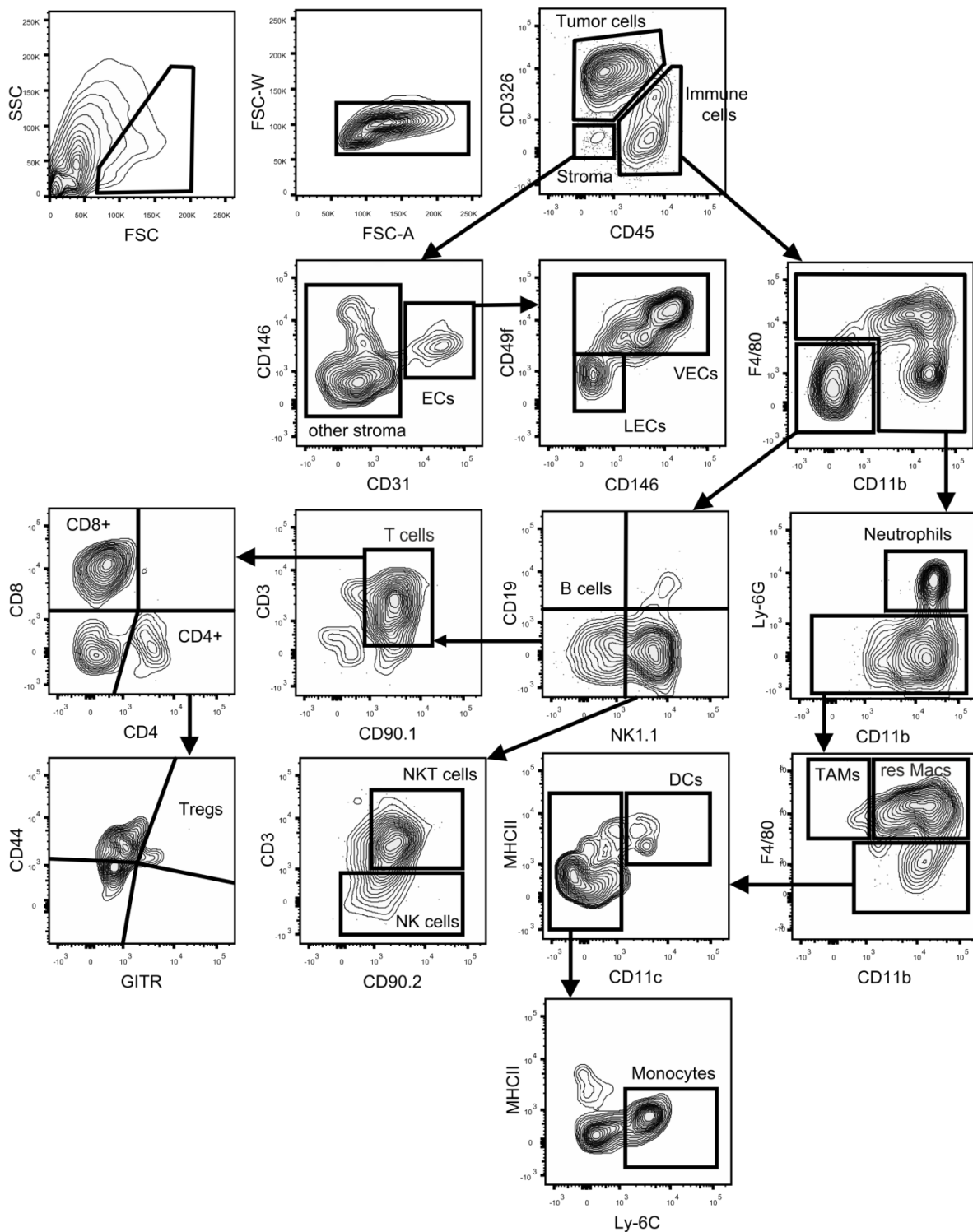


Figure S1 Gating strategy for tumor immune cells. First, viable cells and cell doublets were discriminated by their SSC and FSC characteristics. Single cells were classified as tumor cells (CD326⁺ CD45⁻), stroma (CD326⁻ CD45⁻) and immune cells

(CD326- CD45+). Stroma was further characterized as vascular endothelial cells (VECs, CD326- CD45- CD31+ CD49f+ CD146+/-) and lymphatic endothelial cells (LECs, CD326- CD45- CD31+ CD49f- CD146-). Immune cells were further characterized as neutrophils (CD326- CD45+ Ly-6G+ CD11b+), tumor-associated macrophages (TAMs, CD326- CD45+ Ly-6G- F4/80+ CD11blow), resident macrophages (res Macs, CD326- CD45+ Ly-6G- F4/80+ CD11bhigh), DCs (CD326- CD45+ Ly-6G- F4/80- CD11b+ MHCII+ CD11c+), monocytes (CD326- CD45+ Ly-6G- F4/80- CD11b+ MHCII- CD11c- Ly-6C+), B cells (CD326- CD45+ F4/80- CD11b- CD19+), NK cells (CD326- CD45+ F4/80- CD11b- NK1.1+ CD3- CD90.2+/-), NKT cells (CD326- CD45+ F4/80- CD11b- NK1.1+ CD3+ CD90.2+), T cells (CD326- CD45+ F4/80- CD11b- CD19- NK1.1- CD90.2+ CD3+), TH cells (CD326- CD45+ F4/80- CD11b- CD19- NK1.1- CD90.2+ CD3+ CD4+), regulatory T cells (Tregs, CD326- CD45+ F4/80- CD11b- CD19- NK1.1- CD90.2+ CD3+ CD4+ CD44+ GITR+) and cytotoxic T cells (CD8+, CD326- CD45+ F4/80- CD11b- CD19- NK1.1- CD90.2+ CD3+ CD8+). Representative contour plots from a WT PyMT tumor are shown.

Supplemental Figure 2:

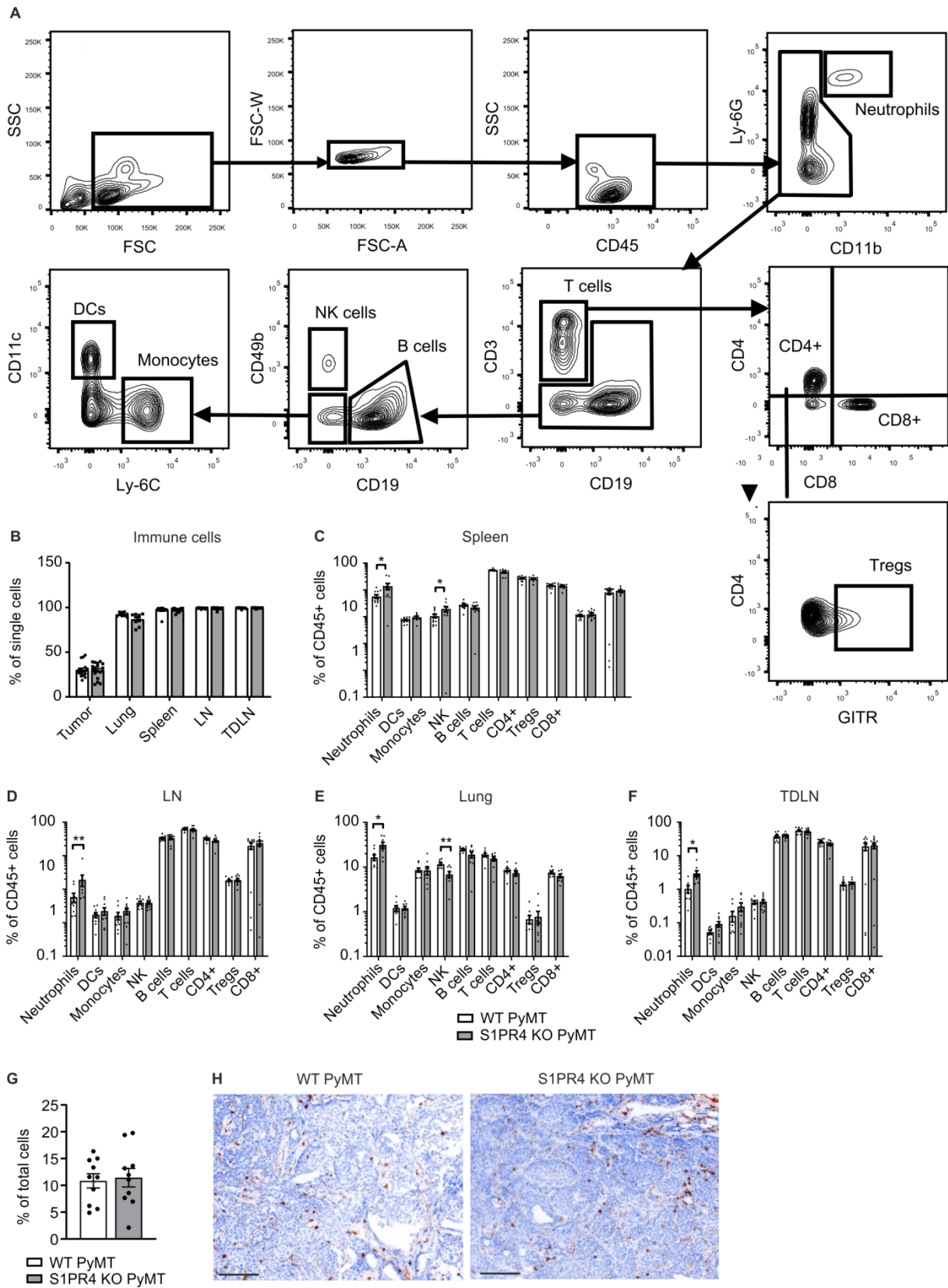


Figure S2 Immune cell profiles of spleen, LNs, TDLNs and lungs of WT vs. S1PR4 KO PyMT mice. (A) Gating strategy for spleen, mesenteric LN, lung and TDLN of WT vs. S1PR4 KO PyMT mice. First, viable cells and cell doublets were discriminated by their SSC and FSC characteristics. Next, all living immune cells were identified (SSC^{low} CD45⁺) and the following subpopulations defined: neutrophils (CD11b⁺ Ly-6G⁺), T cells (CD11b⁻ Ly-6G⁻ CD3⁺), Th cells (CD11b⁻ Ly-6G⁻ CD3⁺ CD4⁺), regulatory T cells (Tregs, CD11b⁻ Ly-6G⁻ CD3⁺ CD4⁺ GITR⁺), cytotoxic T cells (CD11b⁻ Ly-6G⁻ CD3⁺ CD8⁺), B cells (CD11b⁻ Ly-6G⁻ CD3⁻ CD19⁺), NK cells (CD11b⁻ Ly-6G⁻ CD3⁻ CD49b⁺), monocytes (CD11b⁻ Ly-6G⁻ CD3⁻ CD49b⁻ CD19⁻ Ly-6C⁺) and dendritic cells (DCs, CD11b⁻ Ly-6G⁻ CD3⁻ CD49b⁻ CD19⁻ CD11c⁺). Representative contour plots from a WT PyMT spleen are shown. (B) Relative amounts of total CD45⁺ immune cells in tumor, lung, spleen, LN and TDLN from WT and S1PR4 KO PyMT mice are shown. (C - F) Relative amounts of myeloid cell and lymphocyte subsets in spleen (C), LN (D), lung (E) and TDLN (F) from WT and S1PR4 KO PyMT mice were determined by flow cytometry. (G, H) Sections from WT and S1PR4 KO tumors were stained for CD45. (G) Quantification of CD45⁺ cells in WT and S1PR4 KO (n = 10 each) tumor sections as percentage per total cells. (H) Representative sections from WT and S1PR4 KO tumors were stained for CD45 (brown) to indicate immune cells and DAPI (blue) to counterstain nuclei. Scale bars represent 200 μ m. Data are means \pm SEM. p values were calculated using two-tailed Student's t test. *p<0.05, **p<0.01.

Supplemental Figure 3:

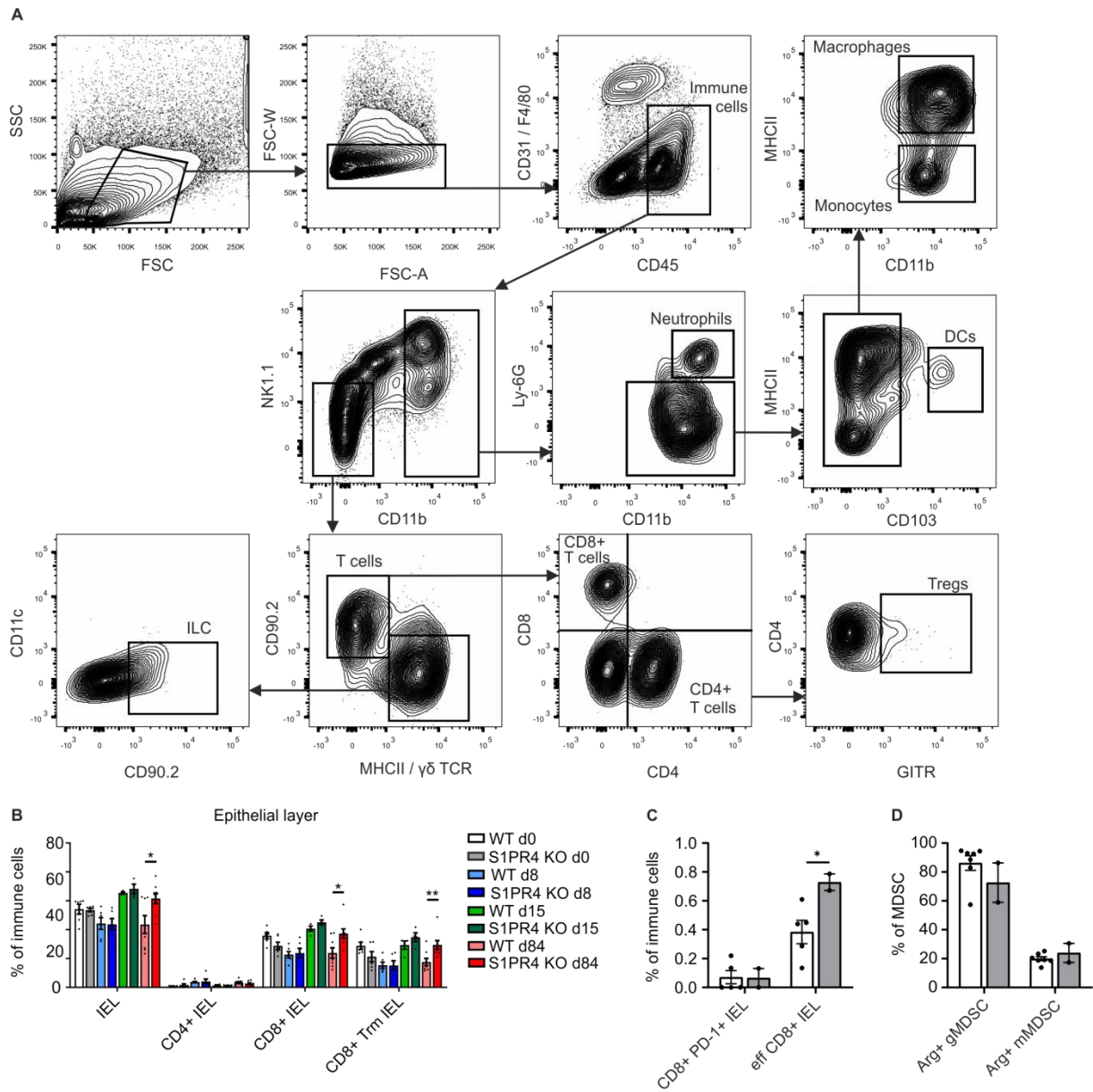


Figure S3 Immune profile of colon epithelium and lamina propria. (A) Gating strategy for murine lamina propria and epithelium. First, viable cells and cell doublets were discriminated by their SSC and FSC characteristics. Single cells were classified as immune cells (CD31- CD45+) and further characterized as neutrophils (CD31- CD45+ Ly-6G+ CD11b+), DCs (CD31- CD45+ Ly-6G- CD11b+ MHCII+ CD103+), macrophages (CD31- CD45+ Ly-6G- CD11b+ MHCII+), monocytes (CD31- CD45+ Ly-6G- CD11b+ MHCII-), T cells (CD31- CD45+ CD11b- NK1.1- CD90.2+ MHCII-), CD4+ T cells (CD31- CD45+ CD11b- NK1.1- CD90.2+ MHCII- CD4+), CD8+ T cells (CD31- CD45+ CD11b- NK1.1- CD90.2+ MHCII- CD4- CD8+), and Tregs (CD31- CD45+ CD11b- NK1.1- CD90.2+ MHCII- CD4+ GITR-).

T cells (CD31- CD45+ CD11b- NK1.1- CD90.2+ MHCII- CD4+), regulatory T cells (Tregs, CD31- CD45+ CD11b- NK1.1- CD90.2+ MHCII- CD4+ GITR+), cytotoxic CD8+ T cells (CD31- CD45+ CD11b- NK1.1- CD90.2+ MHCII- CD8+) and innate lymphoid cells (ILC, CD31- CD45+ CD11b- NK1.1- MHCII+ $\gamma\delta$ TCR+ CD90.2+). Representative contour plots from a WT colon (d84) are shown. (B) Relative amounts of immune cell populations within the epithelial layer of WT and S1PR4 KO mice at day 0, day 8, day 15 and day 84 analyzed by polychromatic flow cytometry. (C) Relative amounts of exhausted (PD-1+) and effector CD8+ IEL (CD49a- CD103-) in the epithelial layer of WT and S1PR4 KO colons at d84 determined by flow cytometry. (D) Relative amounts of gMDSCs (CD11b+ Ly6Ghigh Ly6Clow) and mMDSCs (CD11b+ Ly6Glow Ly6Chigh) stained intracellularly for arginase 1 (Arg1) in lamina propria of WT and S1PR4 KO mice at d84 determined by flow cytometry. Data are means + SEM. p values were calculated using two-tailed Student's t test. *p<0.05, **p<0.01.

Supplemental Figure 4:

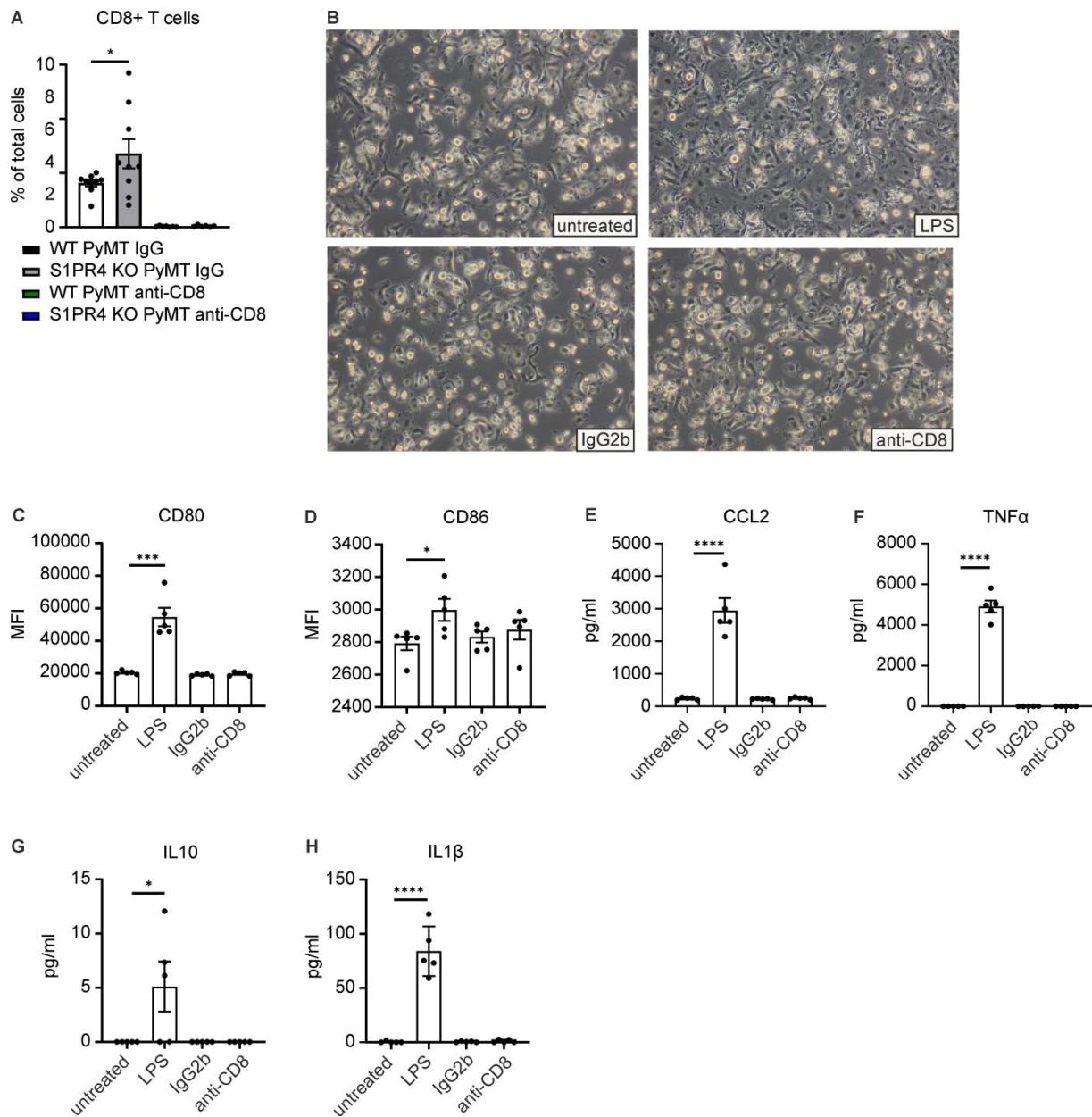


Figure S4 IgG antibodies used for in vivo studies do not activate bone marrow-derived macrophages. (A) Relative amounts of CD8+ T cells infiltrated into tumors from DXR-treated PyMT WT mice treated with IgG2b isotype control or anti-CD8 antibody, or DXR-treated S1PR4 KO PyMT treated with IgG isotype control and anti-CD8 5 weeks after initial treatment. (B-H) Bone marrow-derived macrophages (BMDM) were stimulated with LPS (50 ng/ml), IgG2b isotype control or anti-CD8 antibodies (50 μ g/ml each) for 24 h. (B) Morphological changes were determined by light microscopy.

Expression of CD80 (C) and CD86 (D) was assessed by FACS and mean fluorescence intensity (MFI) is shown. Concentrations of CCL2 (E), TNF α (F), IL-10 (G) and IL1 β (H) were determined by cytometric bead array from supernatants of stimulated or untreated BMDM. Data are means \pm SEM. p values were calculated using two-tailed Student's t test. *p<0.05, ***p<0.001, ****p<0.001.

Supplemental Figure 5:

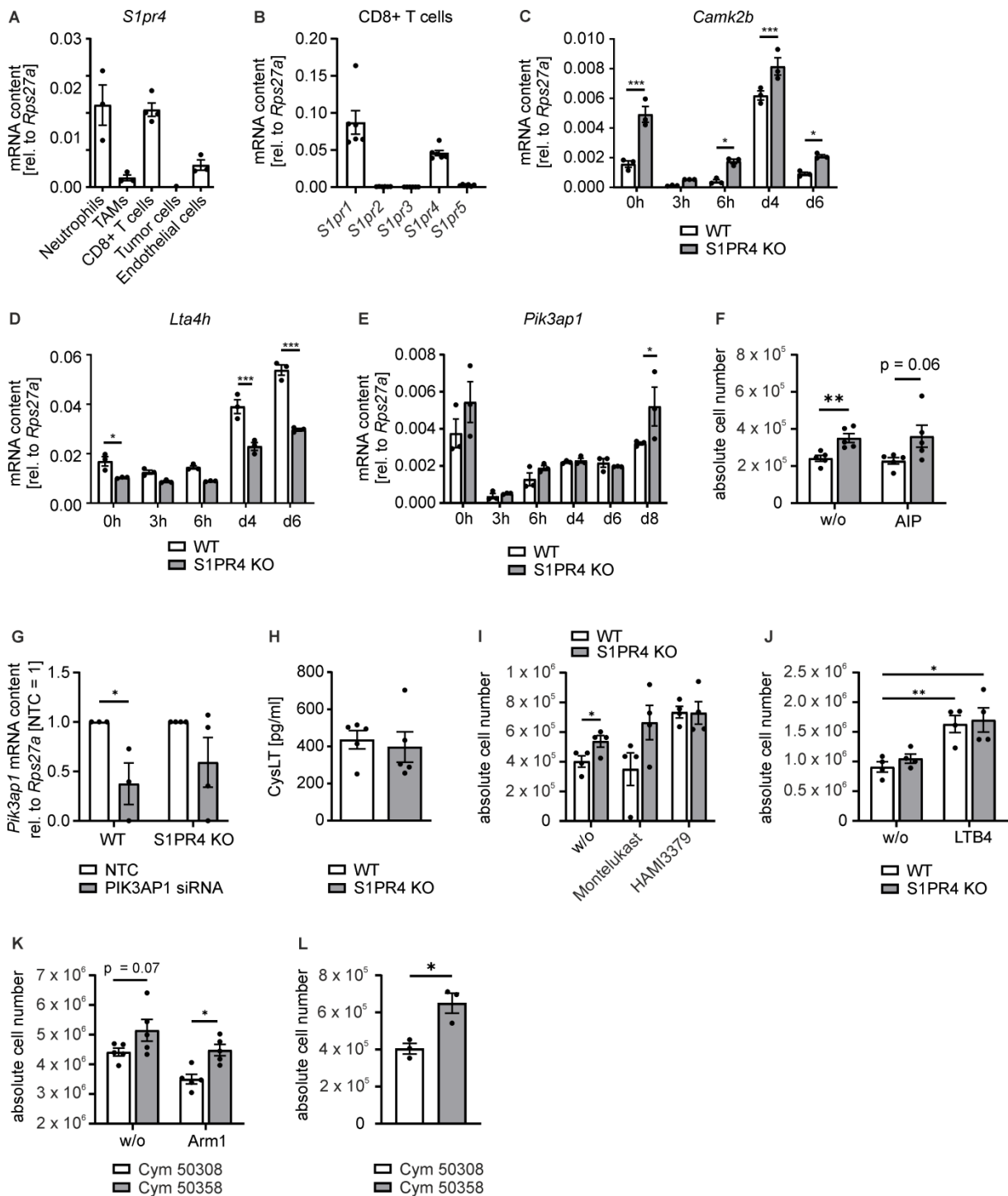


Figure S5. S1PR4 gene expression profile and CD8+ T cell target validation in vitro. (A) Expression of *S1pr4* mRNA by neutrophils, tumor-associated macrophages, CD8+ T cells, tumor cells and endothelial cells FACS-sorted from WT PyMT tumors was determined by qPCR. (B) *S1pr1-5* expression in CD8+ T cells isolated from

spleens of untreated WT mice determined by quantitative PCR. (C-E) Expression of selected target genes *Camk2b* (C), *Lta4h* (D) and *Pik3ap1* (E) in WT and S1PR4 KO CD8+ T cells 0h, 3h, 6h, 4d and 6d after activation determined by quantitative PCR. (F) Absolute cell number of WT and S1PR4 KO CD8+ T cells at day 2 either untreated (w/o) or treated with 5 μ M CAMK2 inhibitor (AIP). (G) Expression of *Pik3ap1* in non-target control (NTC) and PIK3AP1 siRNA treated CD8+ WT and S1PR4 KO T cells determined by quantitative PCR. NTC was set to 1. (H) Concentration of cysteinyl leukotrienes (LTC₄, LTD₄, LTE₄) in supernatants of WT and S1PR4 KO CD8+ T cells 2 days after activation determined by ELISA. (I) Absolute cell number of WT and S1PR4 KO CD8+ T cells at day 3 either untreated (w/o) or treated with 8 μ M of CysLT1R inhibitor (Montelukast) or 4 μ M of CysLT2R inhibitor (HAMI3379). (J) Absolute cell number of WT and S1PR4 KO CD8+ T cells at day 3 either untreated (w/o) or treated with 100 nM of LTB₄. (K) Absolute cell number of WT and S1PR4 KO CD8+ T cells either untreated (w/o) or treated with 5 μ M Arm1 5 days post-activation. (L) Absolute cell number of WT and S1PR4 KO CD8+ T cells either treated with 200 nM S1PR4 agonist (Cym 50308) or S1PR4 antagonist (Cym 50358) 4 days post-activation. Data are means + SEM. p values were calculated using two-way ANOVA with Bonferroni's correction (C-E) or two-tailed Students t-test (F, G, I-L). *p<0.05, ***p<0.001.

Supplemental Figure 6:

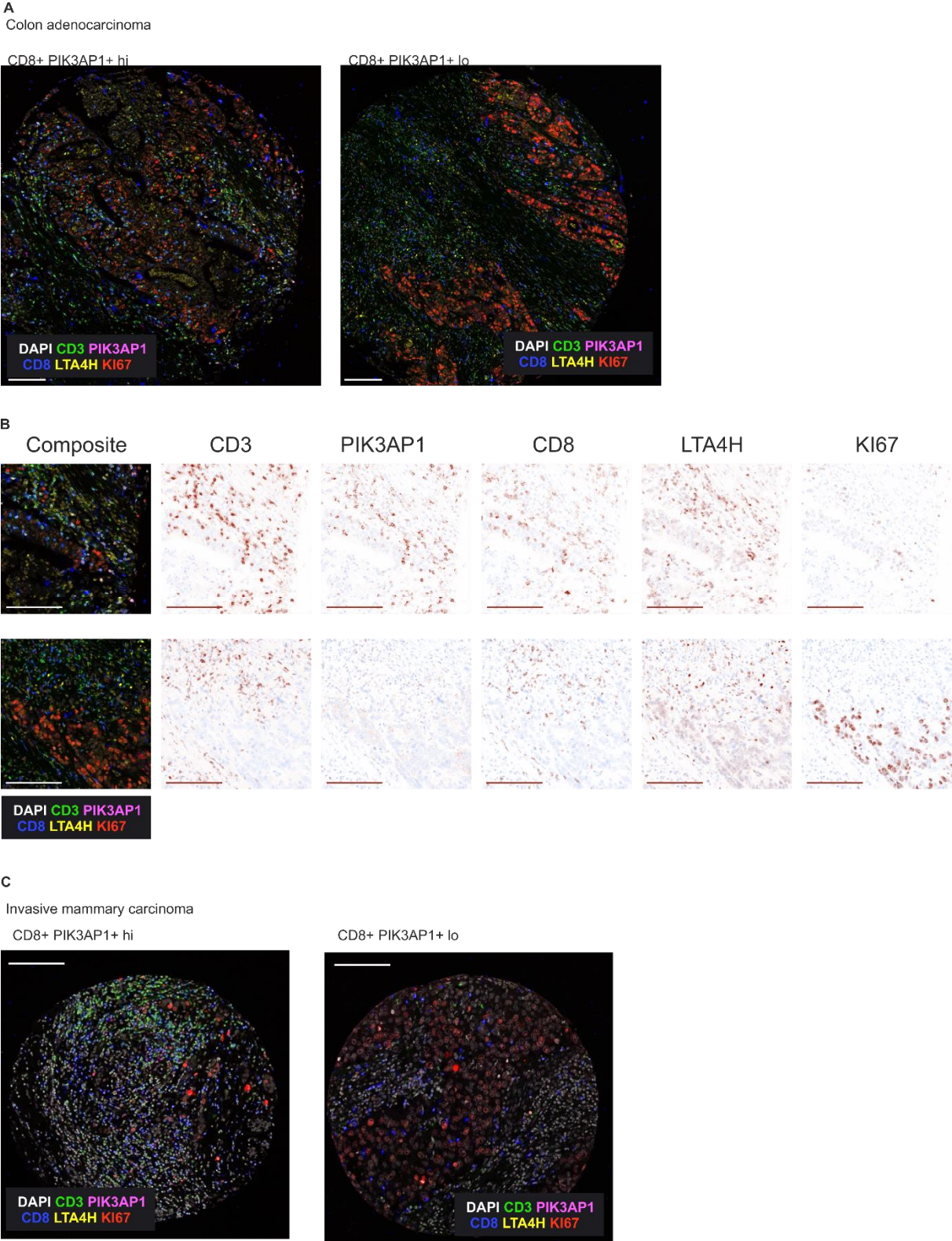


Figure S6. PhenOptics multispectral immunostaining of tissue cores from colon adenocarcinoma and mammary carcinoma patients. Tissue microarrays of human

colon adenocarcinoma (A, B) and human invasive mammary carcinoma (C) cores were stained for CD3, CD8, PIK3AP1, LTA4H and KI67 by PhenOptics. Nuclei were counterstained with DAPI. (A) Complete colon adenocarcinoma cores and (B) full as well as single stainings of the magnified areas shown in Figure 5H computed using InForm software. (C) Representative images of invasive mammary carcinoma tissue cores. Scale bars represent 100 μm .

SUPPLEMENTAL MATERIAL AND METHODS

Flow cytometry

For characterization of immune cell subsets in tumors, lungs, LNs, TDLNs, spleens and colons the following antibodies were used: anti-CD3-PE-CF594 (145-2C11), anti-CD4-BV711 (GK1.5) or anti-CD4-V500 (RM4-5) (for organs), anti-CD11c-BV711 (HL3) or anti-CD11c-AlexaFluor700 (HL3) (for organs), anti-CD19-APC-H7 (1D3), anti-CD25-PE-Cy7 (BD Biosciences, PC61) (for organs), anti-CD34-FITC (RAM34), anti-CD44-AlexaFluor700 (IM7), anti-CD49f-PE-CF594 (GoH3), anti-CD140-PE (APA5), anti-CD146-AlexaFluor488 (ME-9F1), anti-CD326-BV711 (G8.8), anti-Ly-6C-PerCP-Cy5.5 (AL-21), anti-NK1.1-BV510 (PK136) (all from BD Biosciences), anti-CD8-BV650 (53-6.7), anti-CD11b-BV605 (M1/70), anti-CD324-AlexaFluor647 (DECMA-1), anti-F4/80-PE-Cy7 (BM8), anti-GITR-FITC (DTA-1), anti-Ly-6G-APC-Cy7 (1A8), anti-SiglecH-FITC (551), anti-GDTCR-APC (GL3), anti-CD103-FITC (2E7) (all from BioLegend), anti-CD31-PE-Cy7 (390), anti-CD117-APC-eFluor780 (ACK2) (both from eBioscience), anti-CD45-VioBlue (30-F11.1), anti-CD49b-PE (DX5) (for organs), anti-CD90.2-PE (30-H12), anti-MHCII-APC (M5/114.15.2) (all from Miltenyi).

For characterization of different CD8⁺ T cell subsets single cell suspension were stained with above mentioned anti-CD3, anti-CD8, anti-CD44, anti-CD90.2, anti-CD103, anti-CD4-BV711 and anti-CD11c-BV711 as well as anti-CD45-AlexaFluor (BD Biosciences, 30-F11), anti-PD-1-BV421 (BioLegend, 29F.1A12) and anti-CD49a-PerCP-Cy5.5 (BD Biosciences, Ha31/8).

For characterization of FoxP3⁺ Tregs in PyMT tumors and Arg1⁺ gMDSCs, Arg1⁺ mMDSCs in both tumor mouse models single cell suspensions were stained extracellularly with above mentioned CD3, CD4, CD8, CD11b, CD19, CD25, GITR, Ly-6C, Ly-6G, CD45 and CTLA-4-BV421 (BioLegend, UC10-4B9), MHCII-PE-Cy7

(BioLegend, M5/114.15.2) antibodies before intracellular staining for Arginase 1-APC (Invitrogen, A1exF5) and FoxP3-PE (Invitrogen, FJK-16s) was performed using Foxp3 Transcription Factor Staining Buffer Set (eBioscience) according to manufacturer's instructions.

For FACS-Sorting of primary murine TAMs, neutrophils, CD8+ T cells, endothelial cells, tumor cells single cell suspensions were stained with CD326, CD31, CD45, MHCII, CD11b, F4/80, Ly6G, CD3 and CD8 antibodies as mentioned above. Cell suspensions were filtered through a 30 µm cell strainer, diluted to ideal concentrations for cell sorting, and CD326+ tumor cells, CD31+ endothelial cells, CD11b low F4/80 high TAMs, CD11b high Ly6G high neutrophils and CD8+ T cells were sorted into medium-prefilled (RPMI 1640 plus 10% FCS, 100 U/mL penicillin and 100 µg/mL streptomycin) FACS tubes at 4°C.

Chemokine quantification

To determine the levels of 13 different chemokines in tumor supernatants of WT and S1PR4 KO PyMT mice the LEGENDplex™ mouse proinflammatory chemokine panel was used (Biolegend) according to the manufacturer's instructions. Samples were acquired by flow cytometry and analyzed using FlowJo V10.

Murine primer sequences

For amplifying murine *S1pr1-5* QuantiTect Primer Assays (Qiagen) were used.

Camk2b F: 5'- GCACGTCATTGGCGAGGAT-3', R: 5'- ACGGGTCTCTTCGGACTGG-3'

Ki67 F: 5'-ACCGTGGAGTAGTTTATCTGGG-3', R: 5'-TGTTTCCAGTCCGCTTACTTCT-3'

Lta4h F: 5'- GAGGTCGCGGATACTTGCTC-3', R: 5'- CTCCTGTGACTGGACCGTG-3'

Pik3ap1 F: 5'-AAATGACTTGTGATGATGAGCCA-3', R: 5'-GCTCCGTGTCCGGTTACTGA-3'

Rps27a F: 5'-GACCCTTACGGGGAAAACCAT-3', R: 5'-AGACAAAGTCCGGCCATCTTC-3'

In vitro BMDM differentiation and stimulation

For BMDM differentiation femur and tibia of WT mice were flushed with PBS and cells were filtered through a 70 µm syringe falcon (BD Biosciences) before seeded in 6 Well plates at a density of 4×10^6 cells per well. BMDM were differentiated with 20 ng/µl GM-CSF & M-CSF (both from Peprotech) for 7 days before stimulated with 50 ng/ml LPS, 50 µg/ml anti-CD8 (BioXCell, YTS 169.4) or 50 µg/ml IgG2b (BioXCell, LTF-2) for 24 hrs. Afterwards BMDM were stained with anti-CD80-PE (BioLegend, 16-10A1), anti-CD86-eFluor605 (eBiosciences, GL1), anti-Ly6G-APC-Cy7 (BioLegend, 1A8), anti-MHCII-APC (Miltenyi, M5/114.15.2) and anti-F4/80-PE-Cy7 (BioLegend, BM8). BMDM were identified as F4/80+ MHCII+ Ly6G- population by flow cytometry. Protein levels of CCL2, TNFA, IL10 and IL1B was assessed using Cytometric Bead Array (CBA) Mouse Flex Sets (BD Biosciences) according to manufacturer's instructions.

T cell proliferation assay

CD8+ T cells were isolated from murine spleens using a murine CD8+ T cell Isolation Kit (Stemcell Technologies) and cultured in T cell medium (RPMI 1640, supplemented with 5 mM glutamine, 100 U/ml penicillin, 100 µg/ml streptomycin, 10% heat-inactivated FCS, 1% nonessential and essential aminoacids, 1% sodiumpyruvate and 1% HEPES). 3×10^5 CD8+ T cells were pre-treated with or without 8 µM of CysLT1R inhibitor Montelukast (Cayman Chemical), 4 µM of CysLT2R inhibitor HAMI3379 (APEX BIO) or 100 nM LTB4 (Cayman Chemical) for 30 min before activated with mouse T activator CD3/CD28 Dynabeads (Thermo Fisher Scientific) and cultured for indicated times. CysLT protein levels were determined by ELISA (Enzo Life Sciences).